Perveance and ion bunch structure from a "compact, high-pressure" laser ion source

P. Yeates,[1] J. T. Costello,[1,2] and E. T. Kennedy[1,2]
[1]*National Centre for Plasma Science and Technology (NCPST), Dublin City University (DCU), Dublin, Ireland*
[2]*School of Physical Sciences, Dublin City University (DCU), Dublin, Ireland*

(Received 30 September 2010; accepted 23 November 2010; published online 13 December 2010)

The Dublin City University (DCU) laser ion source (LIS) is a "compact high-pressure" laser ion source utilizing a table top Q-switched laser. The DCU-LIS combines high laser fluence ($F>4$ kJ cm^{-2}), high laser intensity ($I>10^{11}$ W cm^{-2}) with a short field free region ($L=48$ mm) and high source potential ($V_{ext}>40$ kV) in order to offset recombination losses within the plasma and maximize the proportion of highly charged ions which are extracted from the plasma plume. Such a configuration also provides high peak currents ($I_p>3$ mA), high current densities ($J>5$ mA cm^{-2}), and high charge states (Cu^{6+}) in the extracted ion-bunch train. However, to obtain and utilize these parameter values in a high pressure LIS requires characterization and control of a number of processes related to ion dynamics and space charge effects on the extracted ions at the plasma plume-anode-extraction gap interface. Relevant issues include electric field distortion, Debye shielding, beam divergence, overfocusing, and perveance (P) in addition to current density profiles for the extracted ion beam. In this paper we focus on these issues and their impact on charge particle extraction and acceleration with a view to elucidating the parameter regimes within which the DCU-LIS performance envelope is optimal. © *2010 American Institute of Physics*.
[doi:10.1063/1.3526738]

I. INTRODUCTION

High intensity laser ($I>10^8$ W cm^{-2}) generated plasmas have, since the early 1960s (Ref. 1) proven to be a valued source of multiply charged ions. Unlike sources such as electron beam ion sources, electron cyclotron resonance ion sources and other electrically generated plasma sources, a laser ion source (LIS) demonstrates high peak current, pulsed operation (advantageous for time resolved applications and accelerator injection) and can produce ions of any element in the periodic table. The performance of a LIS is usually characterized by the peak current (I_p), the average charge state extracted ($\langle Z\rangle$), and the kinetic energy of the extracted ion beam (K_e). Of comparable importance are the beam diameter (and in concert with the peak current, the current density J) and the duration and energy spread of each charge resolved ion bunch. Such parameters constitute the primary indicators of the source's operational capacity.

Laser ion source performance is also strongly determined by the geometry of the system. This is determined by the various apertures present (anode and cathode, drift tube and electrostatic-optics), the total length of the system (including the distance the plasma plume transits before undergoing extraction and electrostatic acceleration, termed the field free region, L) which is mainly composed of the drift tube (of length D) and includes any required intervening energy or charge selective electrostatic optical elements. Traditional LIS systems usually extract charged particles after the plasma plume has undergone free expansion over a distance ranging[2–4] from $L=10$ cm to $L=1.5$ m. The peak (extracted) current is strongly dependent on this distance ($I_p \propto 1/L^3$) and one must configure the system design to optimize its operation for the desired application. Ion beams extracted from plasmas have found applications ranging from nanostructure fabrication[5] to compact accelerators for ion implantation[6] material studies for historical analysis[7] and more recently biophysics[8] studies and applications in medical treatments.[9] It has taken nearly two decades to evolve from fundamental studies of highly charged ion generation to cultural, industrial, and medical applications.

A large body of work was undertaken throughout the 1970s and early 1980s to determine the optimal designs for extracting highly charged ions from dense plasma plumes. For example, circular apertures were proven to offer the best peak output current.[10–12] Of special interest was the value of the ratio $s=r/d$, where r is the anode aperture radius and d is the anode-cathode spacing termed the "extraction gap." Reflecting its importance in ion source design, a range of experiments has been undertaken to determine the optimum value of s. Although a number of authors[13–18] have reported s values ranging from 0.36 to 1.4, it was generally found that small values of s (<0.3) led to superior extracted peak current and minimization of beam divergence. The ratio s is also a salient parameter in the design of high power diodes and electron beams.[18–21]

For the most part, authors reporting on the performance of their systems quote variables such as extracted/collected charge, peak current, current density, etc. These are all scalar quantities and do not directly provide information on the beam geometry. Other important parameters regularly quoted when defining the performance of a system are the emittance and the perveance. The geometrical emittance ε (π mm mrad) of a charged particle beam is related to the

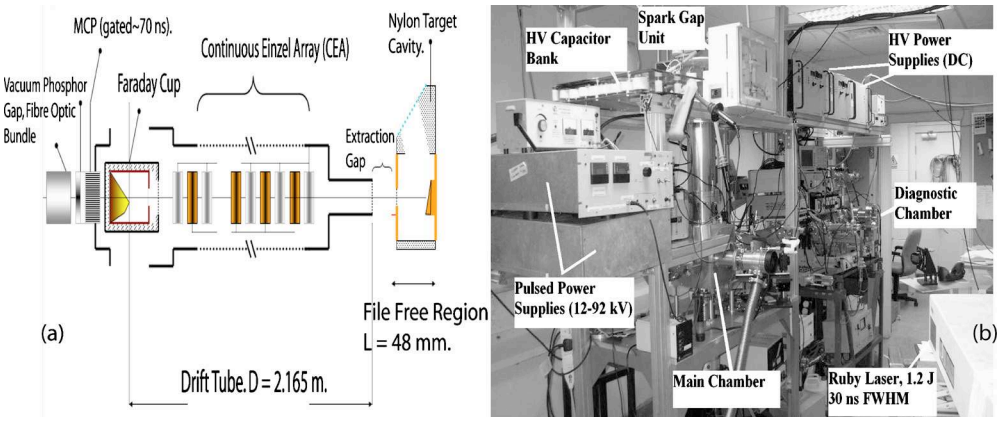

FIG. 1. (Color online) DCU-LIS system. (a) System schematic and (b) system image.

divergence angle and velocities of the particles within the extracted beam. It allows the designer to determine what percentage of the beam falls within a certain radius and it is an extremely valuable parameter as it permits the comparison of beams in widely disparate ion source designs. The perveance P is a measure of the extent to which the space-charge force within an ion beam affects the throughput of the system. Analytically it is given by the expression $P=(I/V^{3/2})$ where I is the peak current and V is the extraction bias. Recorded perveance at the exit aperture of a charged particle source is usually referred to as the "gun perveance" and should be distinguished from the dimensionless value of perveance, measured at the end of a beam transport system and this would include all beam loss mechanisms associated with the system. This variable can be used to quantify the ion source performance, irrespective of the mechanism of plasma production or extraction optics. Finally, the "extraction efficiency" (expected K_e versus the actual K_e) and in parallel with this, the beam transport mechanism determines the structure of the ion beam and the measured current density at some desired target point.

In two previous papers[22,23] we reported on the operation and performance of the DCU-LIS. In this paper, our focus is on further elucidating its observed behavior. To achieve this objective we present data on Debye shielding and its relationship to the observed kinetic energies of the extracted copper ions. In particular we focus on the perveance of this system, which relates directly to two very important behaviors, namely, beam divergence and overfocusing. Finally a detailed analysis of the beam structure in relation to the radial, temporal, and charged resolved current density J for Cu^+ to Cu^{5+} is presented and discussed.

The paper is organized as follows. In Sec. II we describe the main components of the system and its operating parameters. In Sec. III the details of the time of flight (TOF) analysis are presented. The effects of extraction at high density (high-pressure) and its relationship to the Debye length within the extraction gap are discussed. In Sec. IV we present a detailed characterization of the system perveance. The fluence (F), charge and voltage dependent perveance of the system is presented and discussed. Finally in Sec. V analysis of the current density (J) distribution throughout the extracted charge bunch is presented and discussed for all charge states Cu^+-Cu^{5+}.

II. SYSTEM DESIGN

A detailed description of the underlying physics, design, performance, and operation of the DCU-LIS is given elsewhere[22,23] and so only a brief outline is given here. A 1.2 J, Q-switched ruby laser (full width at half maximum, FWHM=30 ns, $\lambda=694$ nm) is focused to a focal spot of approximate diameter 120 μm via a 21 cm focal length planoconvex lens, resulting in power densities P in the range $0.12-2.4\times10^{11}$ W cm^{-2} and fluences F varying from 1.2–8.5 kJ cm^{-2} on the target surface via variation of the laser energy. The target, a copper slab, is inclined at 25° to the axis of the drift tube in order to minimize laser beam "smearing."

Referring to Figs. 1(a) and 1(b). The "prechamber," which is mounted centrally within the main vacuum chamber and in which the target is placed, is composed of a single nylon block, 5 cm wide and 4 cm long, that has been hollowed out. The purpose of using a nonmetallic prechamber to form a field free region is to minimize the surface area which must be biased to some high potential. This reduces arcing at high bias values. At either end of the nylon block copper plates are fixed to act as the target holder and as the anode. The anode aperture is circular and is 6 mm in diameter and covered by five layers of tungsten mesh. Each individual layer is 81% transparent, giving a net (anode) transparency of ~35%. The laser pulse is delivered to the target through a second bore, aligned 45° to the system axis and covered with a glass slide. The volume enclosed by the copper plates constitutes the field free region of the system which has diameter 3.5 cm and length $L=4.8$ cm across which the plasma plume expands upon termination of the laser pulse, subsequently exiting the field free region via the anode aperture. The extraction gap, which is 2.4 cm in width, leads to the cathode. This forms the grounded entrance aperture to the drift tube. The cathode is covered by four layers of tungsten mesh. Thus the total transparency of the anode-cathode system is ~15%. The high density meshes serve two purposes. Firstly, the low transparency places a ceiling on the plasma density

which can enter the extraction gap. This facilitates high fluence and high laser intensity plasma generation in order to maximize the yield of highly charged ions, and importantly, at high source potential for optimal extraction and electrostatic acceleration of these ions. In addition, the high density mesh creates a large number of electrostatic "source" to "sink" points which ensure sufficient field penetration of the plasma plume, and by extension efficient electrostatic acceleration of the plasma ions despite the high N_e present.

Secondly, as will be shown later, a high average charge state within a laser produced plasma inherently results in high N_e, and thus a small Debye length, which affects the coupling between the plasma ions and the electrostatic field within the extraction gap. In turn, distortion of this field, by the plasma bulge at the anode, has a significant influence on the efficiency of extraction and acceleration of charged particles which, as we will see later, is manifested by the turning point in the perveance profile.

Upon exiting the extraction gap, ions are transported down the drift tube (D=2.14 m) to the diagnostic chamber. The drift tube contains an array of Einzel lens units which continuously collimate and focus the ion beam. The electrostatic arrays are required to compensate for the strong space-charge and thermally driven expansion of a high density, highly charged and high velocity plasma plume generated via laser ablation and ionization at the target surface. Because efficient charge separation within the drift tube depends on the extraction voltage (V_{ext}) and the time of flight, both must be maximized. The beam is diagnosed at the end of the drift tube via an irregular geometry enclosed Faraday cup for spatially integrated, time resolved beam current measurements. A scanning planar ion probe, which can transit across the ion beam is used to determine its radial properties. To image the beam structure the system is terminated by a microchannel plate (MCP) phosphor assembly which converts detected ion beam signals to corresponding visible light patterns. These are subsequently imaged via a three-lens system with aperture control onto a charged coupled device (CCD) camera (Pulnix TM-745i) for acquisition via a fast-frame grabber card (EPIX™). The MCP can be operated at a minimum gate width of 70 ns to study the temporal structure of each charge resolved ion bunch.

Finally, to diagnose the plasma signal within the extraction gap an ion probe, consisting of a tungsten wire (length 5 mm and diameter 400 μm, total area 0.04 cm^{-2}) could be placed in front of the cathode to sample the plasma plume directly, albeit, only when high voltage fields were absent.

III. TIME OF FLIGHT ANALYSIS

Electrostatic acceleration is used to separate the different charged states within the extracted ion beam as they transit along the drift tube. The total flight time of an ion is the sum of the drift time in the field free region T_L, the time spent under electrostatic acceleration in the extraction gap T_d, and the flight time in the drift tube, T_D. Thus the total flight time[22] is given by

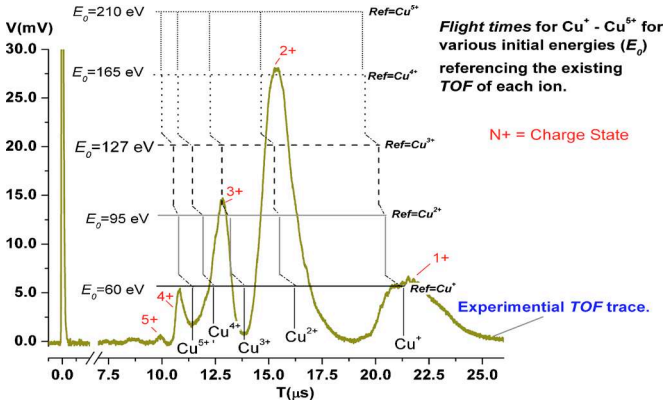

FIG. 2. (Color online) TOF trace from the Faraday cup for an extraction voltage V_{ext}=5 kV laser fluence F=3.9 kJ cm^{-2}. The calculated TOF of each charge resolved ion bunch, when the initial energy E_0 is referenced to a particular ion bunch TOF is also displayed. The Faraday cup bias −150 V.

$$T(U_0,L) = T_L + T_d + T_D. \tag{1}$$

In addition the total potential energy of an ion U with initial energy E_0 is given by

$$U = E_0 + Z_i e d E_d \tag{2}$$

(where the electric field in the accelerating region is given by $E_d = V_{\text{ext}}/d$). Equation (1) can then be rewritten as

$$T(E_0,L) = L\frac{\sqrt{2m_i}}{2\sqrt{E_0}} + \frac{d\sqrt{2m_i}}{\sqrt{E_0}+\sqrt{E_0+Z_i eV}} + \frac{D\sqrt{2m_i}}{2\sqrt{E_0+Z_i eV}}. \tag{3}$$

The only unknown variable in Eq. (3) is E_0, the initial energy of the ions. However for laser plasma generated ions E_0 is not single valued. Hence the TOF of any particular ion bunch is not discrete. In fact, ions of equal charge within a bunch will exhibit a distribution of velocities resulting in a broad TOF profile (Fig. 2). In addition and as previously mentioned, laser plasma plumes can contain ions in high average charge states and consequently Debye shielding will reduce the effectiveness of external electrostatic fields used to accelerate plasma ions and so ion bunches arrive at the Faraday cup with less kinetic energy than would be expected for a particle of charge $Z_i e$ accelerated by a bias of value V_{ext} ($K_E \sim Z_i e V_{\text{ext}}$). These issues result in bunch broadening and yield the partially overlapping TOF curves seen in Fig. 2. This further complicates the process of identification of individual charge states. To overcome this we applied the following procedure.

Referencing Fig. 2 and taking Eq. (3) with V_{ext}=5 kV, the value of E_0 was varied until the calculated TOF of the Cu$^+$ matched the recorded center-of-mass (CM) velocity, for a fluence value of F=3.9 kJ cm^{-2}. The optimum value in this case was 60 eV. This refers to the horizontal line labeled on the right as Ref=Cu$^+$, and on the left at E_0=60 eV (referring to the kinetic energy) in Fig. 2. In this case the calculated TOF of the Cu^{2+} was approximately 15.7 μs, just after the CM point of this ion group. However none of the calculated TOF values for the other ion groups match the CM velocities. The above procedure was repeated, using the

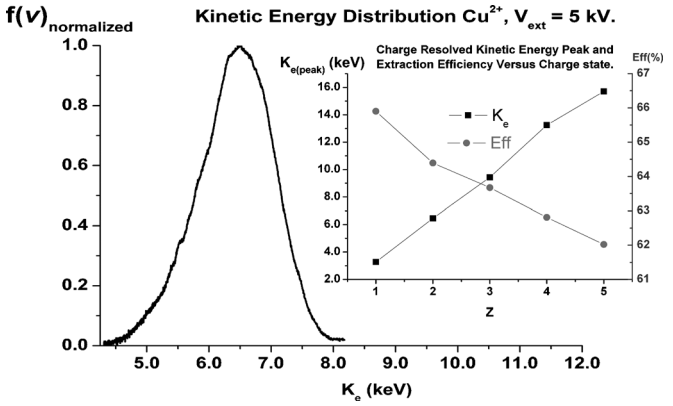

FIG. 3. Normalized kinetic energy distribution of Cu^{2+} vs kinetic energy for V_{ext}=5 kV, F=3.9 kJ cm^{-2}. Inset: extraction efficiency and peak kinetic energy Cu^{+} to Cu^{5+}.

Cu^{2+} CM velocity to determine the optimum value of E_0 so that the calculated TOF of the Cu^{2+} matched the actual CM velocity. This value turned out to be E_0=95 eV. In this instance the calculated TOF of the Cu^{+} remained within the bunch temporal profile for that ion group, but was now shifted ahead of the CM position. Repeating this procedure for high charge states resulted in even higher values for E_0 (up to 210 eV). This iterative procedure allows the assignment of peaks Cu^{+} to Cu^{5+}, respectively.

A second issue is the actual kinetic energy of the beam relative to that expected for a particular value of V_{ext}. In order to study this phenomenon the time dependent current trace must be converted to a kinetic energy distribution plot. This can be done[24] using Eq. (4),

$$f(v) = \frac{I_n(t) \times t^3}{Z_i e m_i D^2}, \tag{4}$$

where D is the drift tube length, $I_n(t)$ is the time dependent current for an ion of charge state n, t is time, Z_i is the charge state, and m_i is the ion mass. The velocity dependent function $f(v)$ is usually normalized to unity.

The time dependent current trace of the Cu^{2+} ion bunch was converted via Eq. (4) to a kinetic energy plot. This is displayed in Fig. 3. It is immediately apparent that the CM kinetic energy of this ion bunch lies in the range 6.3–6.6 keV and not the expected 10 keV$\sim(Z_i e V_{ext})$. The ratio of the actual to expected kinetic energy gives an approximate "extraction efficiency" of ~63%. When this procedure is applied to all ion groups (Cu^{+} to Cu^{5+}), extraction efficiencies of 61%–67% are obtained (see inset Fig. 3). Extraction efficiencies in this range can be considered very good, as values as low as 30% have been reported for some laser ion sources.[25]

These issues are of great importance in TOF studies. As a TOF spectrum becomes more complex then the difficulties and errors involved in charge state identification increase. With increasing laser intensity the maximum charge state which can be generated increases. To effectively separate the various charge resolved bunches one must utilize a longer drift tube to allow for sufficient TOF dispersion and concomitant increased charge separation. This creates various issues regarding beam transport, beam loss due to space-charge driven radial beam expansion and ion collisions with the ambient atmosphere.

TABLE I. Reference ion, E_0, and E_0/Z_i.

Cu^{n+}	E_0 (eV)	E_0/Z_i (eV)
Cu^{+}	60.00	60.00
Cu^{2+}	95.00	47.50
Cu^{3+}	127.00	42.33
Cu^{4+}	165.00	41.25
Cu^{5+}	210.00	42.00

One can also use higher extraction voltages to improve the separation of successively charged ion bunches over a shorter drift tube. However the maximum extraction bias which can be utilized is constrained by arcing when the plasma conductivity exceeds a critical value. Interestingly, the optimum initial energy E_0 used to determine the TOF of each ion converges to ≈40 eV per charge state (cf., Table I). This would imply that the initial energy of the plasma, upon termination of the laser pulse, is close to this value. In reality, increasing the extraction voltage for a plasma plume with sufficiently high electron density to create strong Debye shielding will certainly lead to distortion of the bias field in the extraction gap and result in beam loss due to over focusing upon injection into the drift tube.

In order to diagnose the properties of the extracted plasma within the extraction gap, the ion wire probe was used to acquire time dependent voltage traces of the ion signal for a range of fluences when no extraction field was present. The ion density $N_i(t)$ within the extraction gap can be calculated using the time dependent current signal[26] I_T from the probe tip via the equation

$$N_i(t) = \frac{I_T(y)}{eAv_0}. \tag{5}$$

Here, $A=2rl$ is the projected area of the probe tip of radius r and length l, while v_0 is the velocity of the peak of the ion signal. Figure 4 displays the peak N_i value recorded for each laser fluence and the inset displays the TOF ion current trace for F=3.96 kJ cm^{-2}. The most important variable on which electrodynamics of the plasma ions within the extraction gap depends is the Debye length, λ_D. To determine its value, the electron density N_e and electron temperature T_e are required. The peak N_e value for the range of laser fluences that apply here can be approximated by assuming an average charge state within the plumes of $\langle Z\rangle$=2.5 and converting the time dependent ion density traces to time dependent electron density traces.

In relation to the electron temperature, in a previous publication[22] the time dependent trace I_T was fitted with a function which allowed the plasma temperature T_{KL} (Knudsen layer temperature) and drift velocity to be determined, assuming a shifted Maxwell–Boltzmann ion velocity profile. For "late-stage" adiabatic free expansion we assume that the deduced Knudsen layer $T_{KL} \approx T_i \approx T_e$. Using these

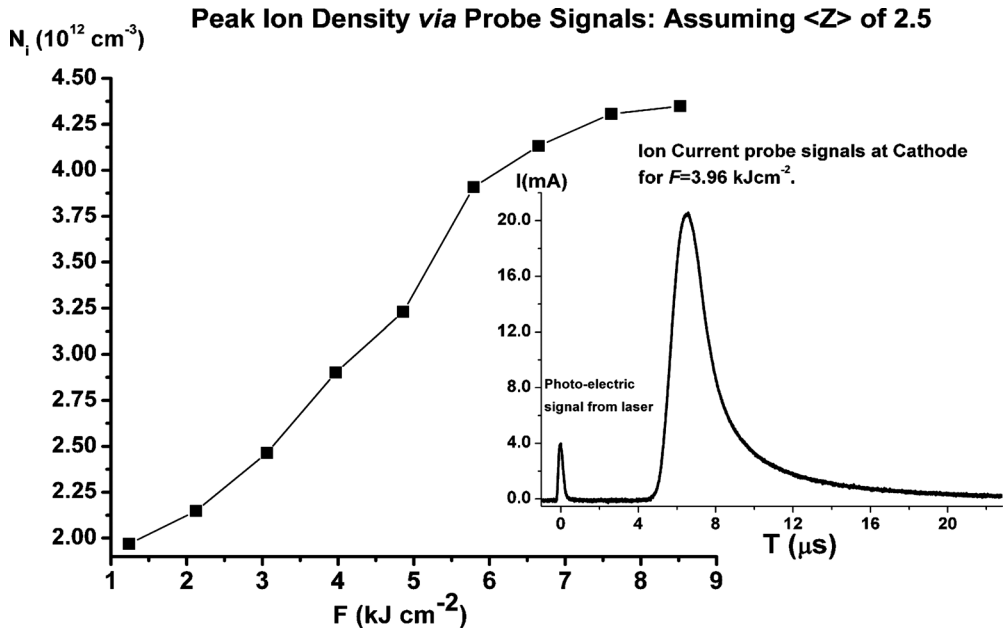

FIG. 4. Measured peak ion density N_i within the extraction gap for all fluences studied. Inset: time dependent current trace from the ion probe, for $F=3.96$ kJ cm^{-2}.

assumptions we can approximate the Debye length[27] to determine the extent of shielding of the plasma ions from the extraction field using equation

$$\lambda_D = \left(\frac{\varepsilon_0 \kappa T_e}{N_e e}\right)^{1/2} = 0.69\left(\frac{T_e}{N_e}\right)^{1/2}. \quad (6)$$

Table II displays the delivered laser intensity, fluence, fitted Knudsen layer temperature, approximate peak N_e, and calculated Debye length. Table II clearly indicates that the Debye length within the plasma plume is substantially less than the dimensions of the extracted plume for all delivered laser fluences This analysis confirms the trends observed in Fig. 3, i.e., the final kinetic energy of the extracted ions is not completely determined by the relation $Z_i e V_{\text{ext}}$, but is in fact a fraction of this quantity (here ~0.65). This result stems directly from the design configuration of the DCU-LIS and the concept of extraction at "high-pressure," close to the plasma generation point.

IV. PERVEANCE

The perveance P provides a measure of the extent to which the flow pattern of a charged particle beam is influenced by space charge and is given by the simple expression $P=I/V^{3/2}$, where I is the extracted beam current and V is the extraction voltage[28] (V_{ext}). A large perveance value means a high proportion of the beam particles are in a normal flow and thus exhibit low divergence. The fundamental limitation on the perveance of a beam is the space-charge limited current. The reported formulation of the current-limit for different ratios of extraction aperture radius r to extraction gap length d varies greatly.[29–31] However as a means of direct comparison of a diverse range of ion sources it is a useful parameter.

A. Derivation of perveance condition

Determination of the current from a parallel plate diode based charge source is based on flow solutions to Poisson's equation ($\nabla^2 V=\rho/\varepsilon_0$) for a one dimensional diode with extraction voltage V_{ext} and space-charge limited flow of density ρ. Its current density is governed by the Child–Langmuir[32] law

$$\frac{I_b}{A} = J_C = \frac{4\varepsilon_0}{9}\sqrt{\frac{2Z_i e}{m_i}}\frac{V_{\text{ext}}^{3/2}}{d^2}. \quad (7)$$

Here $A=\pi r^2$ is the area of the first extraction aperture, m_i is the ion mass, Z_i is the ion charge state, ε_0 is the permittivity of free space, and d is the extraction gap width (SI units). Dividing both sides by $V_{\text{ext}}^{3/2}$ and rearranging gives

TABLE II. Laser intensity, laser fluence, fitted plasma temperature (T_{KL}), peak electron density (N_e), and the Debye length (λ_D).

I (W cm^{-2}) $\times 10^{11}$	F (kJ cm^{-2})	T_{KL} fit (K)	Peak N_e (10^{12} cm^{-3})	λ_D (10^{-6} m)
0.35	1.24	8500	4.92	45.3
0.61	2.12	10 100	5.37	47.3
0.87	3.10	10 450	6.16	44.9
1.13	3.97	10 800	7.25	42.0
1.39	4.86	11 175	8.07	40.5
1.65	5.79	11 500	9.77	37.4
1.90	6.64	12 500	10.03	37.9
2.18	7.61	14 550	10.77	40.1
2.44	8.52	16 600	10.87	42.6

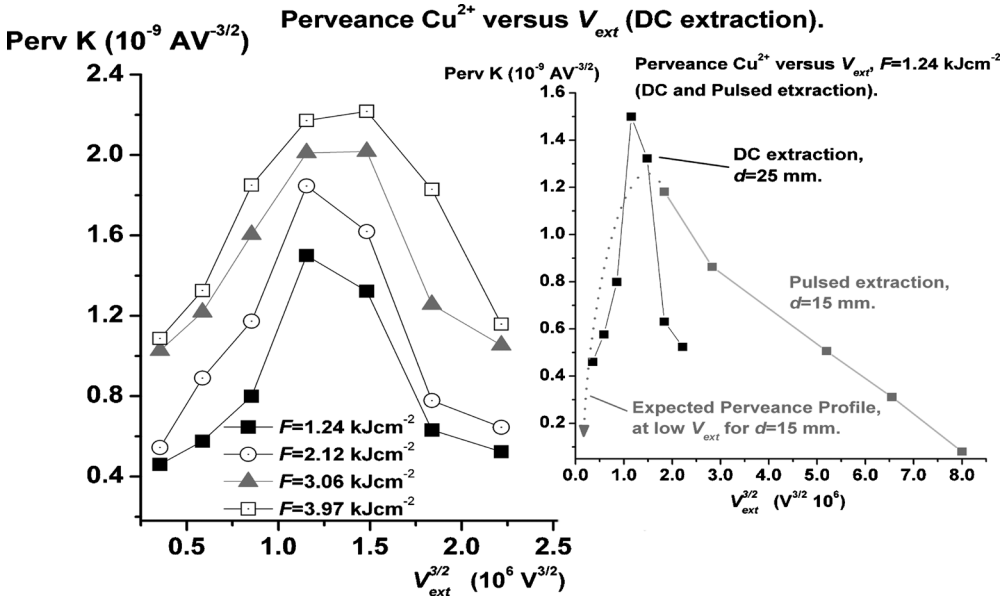

FIG. 5. Measured perveance P for Cu^{2+}. F varies from 1.24 to 3.96 kJ cm^{-2} for dc extraction (5–17 kV). Inset: comparison of perveance profiles for dc (5–17 kV, $d=25$ mm) and pulsed extraction (15–40 kV, $d=12$ mm). The dotted line in the inset outlines the expected perveance profile if pulsed extraction was performed at lower voltages.

$$\sqrt{\frac{m_i}{Z_i}}\frac{I_b}{V_{\text{ext}}^{3/2}} = \sqrt{2}e\frac{4\varepsilon_0\pi}{9}\left(\frac{r}{d}\right)^2. \tag{8}$$

Substituting m_i with $A_i u$ where A_i is the atomic mass of the ion and u is the atomic mass unit and calculating the numerical values of the other constants we obtain

$$\sqrt{\frac{A_i}{Z_i}}\frac{I_b}{V_{\text{ext}}^{3/2}} = 1.72 \times 10^{-7}\left(\frac{r}{d}\right)^2. \tag{9}$$

Thus the perveance P of a system is defined by the ratio of the radius of the extraction aperture to the length of the extraction gap. The design of the beam optics for extraction is constrained by this ratio. Typically, the aspect ratio is kept below a value of 0.5 in order to prevent spherical aberration at the periphery of the beam[32] so that the maximum beam current I_b of a diode with good optics is determined only by the extraction voltage and does not directly depend on the actual diode size. In practice, the beam current increases with diode size because a larger diode can withstand a higher extraction voltage, in contrast the current density decreases with increasing diode diameter.

Given the constant value of r/d, perveance should also be constant in time; however in reality this is rarely the case. The perveance of a system as given by Eq. (9) is termed the

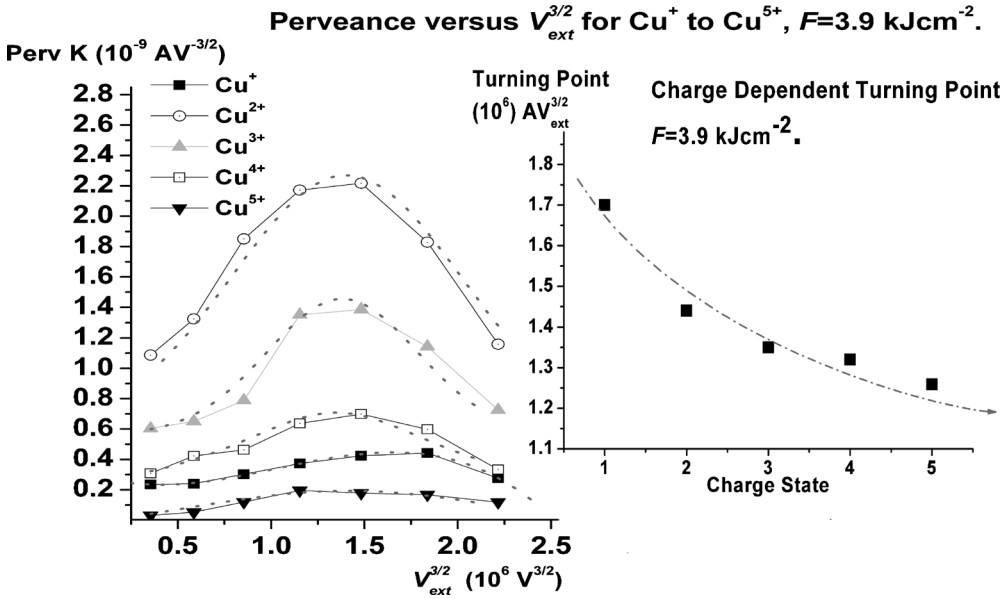

FIG. 6. Perveance P for Cu^{+} to Cu^{5+} for all dc extraction bias values and $F=3.96$ kJ cm^{-2}. Inset: observed turning points in the perveance profiles for each charge state.

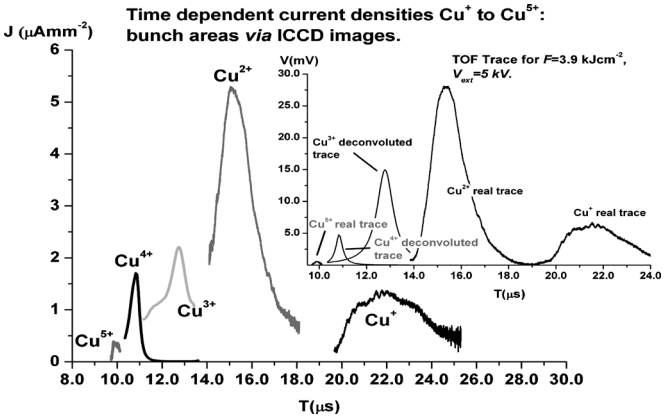

FIG. 7. Time resolved current density traces J, for each charge resolved ion bunch. Currents from the Faraday cup were converted to current densities J using the ion bunch diameter obtained from the corresponding time resolved image. Inset: TOF voltage trace on the Faraday cup for $V_{ext}=5$ kV, $F=3.9$ kJ cm^{-2}.

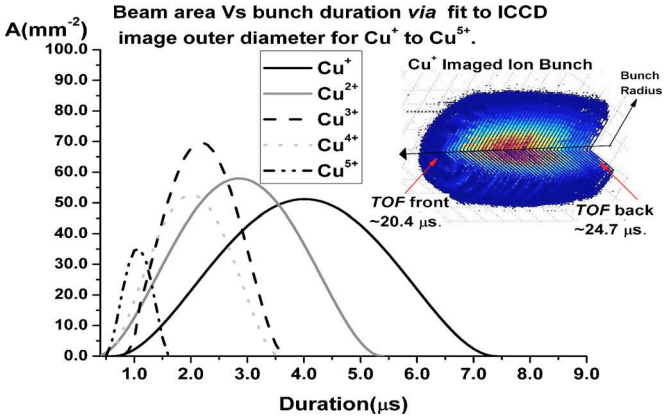

FIG. 8. (Color online) Time resolved area of each ion bunch, Cu^+ to Cu^{5+}, calculated by referencing the outer diameter of the time resolved ICCD images for each ion bunch. (Inset) Mosaic of the time resolved 2D images of the Cu^+ ion bunch, with the upper right quadrant removed to display the detected ion gradient from bunch outer edge to bunch center.

Child–Langmuir perveance P_0 for a plane diode. It has been shown experimentally that the perveance for which the beam divergence is a minimum is in fact a fraction of the Child–Langmuir perveance. Under such conditions an ion beam is termed perveance matched and P takes the value[33,34]

$$P_{optm} = 0.6P_0. \tag{10}$$

The simple linear optics mode of Green[33] assumes that the plasma boundary is a section of an unaberrated, concave spherical surface. The disagreement between the predicted perveance match condition and the reported data would indicate that the true plasma boundary shape is more complex. Numerous authors have addressed deviations from theory but most have done so only for high perveance systems ($P>10^{-6}$ AV$^{-3/2}$) such as electron guns with rigid emitting surfaces.[35–37] In these papers, perveance deviations from the expected values were attributed to the "anode hole" effect.[38] In real extraction systems, the gap length d between the electrodes (usually $>10-15$ mm) is chosen in concert with the desired focal length f of the source using the relationship[39]

$$r/\alpha = f = d \tag{11}$$

(where α is the beam divergence). This expression assumes that no beam transport is required, which is usually not the case for the vast majority of reported experimental systems. In addition, for an expanding plasma plume, the plasma boundary is akin to a dynamic fluid in constant motion and thus the electric field normal to its surface is zero.[39] As a result of the varying plasma boundary and plasma density, the shape of the field in the extraction gap is strongly modified which has a pronounced effect on the performance of both ion source and beam transport systems. In experimental perveance measurements, it is possible for a beam to be overmatched ($P>P_0$) and under such conditions an ion beam can become hollow, while for the undermatched condition ($P<P_0$) the beam can display low distortion, but the current density at its center becomes partially reduced, leading to a double peak radial profile in the current density.[40]

Across a wide range of charge particle generation systems, quoted perveance values show variation over several orders of magnitude. For plasma based ion sources, P can range from 1×10^{-8} AV$^{-3/2}$ (rf gas source)[41] through 2.1×10^{-8} AV$^{-3/2}$ (H^- magnetic multipole ion source)[40] to 7×10^{-8} AV$^{-3/2}$ (duopigatron).[34] For more rigid, high powered devices the perveance ranges from values of $P=6\times10^{-6}$ AV$^{-3/2}$ (high powered diode)[42] through 2×10^{-6} AV$^{-3/2}$ (high powered klystron)[43] to $P>10^{-6}$ AV$^{-3/2}$ (Joint European Torus "plug in neutral injectors").[44] The highest perveance values are reported from simple high power diodes[28] ($P\sim10^{-4}$ AV$^{-3/2}$) and wide aperture diameter ($r>2$ cm) He^+ rf sources[45] for which $P\sim10^{-3}$ AV$^{-3/2}$.

B. System performance profile

As Eq. (9) indicates, the perveance of a LIS is strongly determined by the ratio of r/d (anode radius to extraction gap width). Using this equation we can determine the analytical value of the perveance for the DCU-LIS system which is $P=0.6\times10^{-9}$ AV$^{-3/2}$ for Cu^+ or 1.33×10^{-9} AV$^{-3/2}$ for Cu^{5+} with intermediate values for the doubly to quadruply charged species. If experimental values (determined by $I/V^{3/2}$ measurements) exceed this limit then the system performance would be compromised as the beam divergence would exceed the optimal value. Figure 5 displays the perveance of the Cu^{2+} ion bunch for a range of laser fluences for dc extraction at a gap width $d=24$ mm. The measured perveance profile for all laser fluences employed displays a turning point at a value which is reasonably close to the calculated Child–Langmuir perveance value (for Cu^{2+} at a V_{ext} value of ~15 kV). The observed perveance peak then declines sharply in all cases. We associate this behavior with variation in the real extraction gap of width d, which emanates from the distortion of the defined plasma boundary and resulting plasma "bulge" at the anode.[3,22,23,46,47] This results in a decrease in the effective value of d, temporarily increasing the maximum current density J which can be extracted from a parallel plate system.

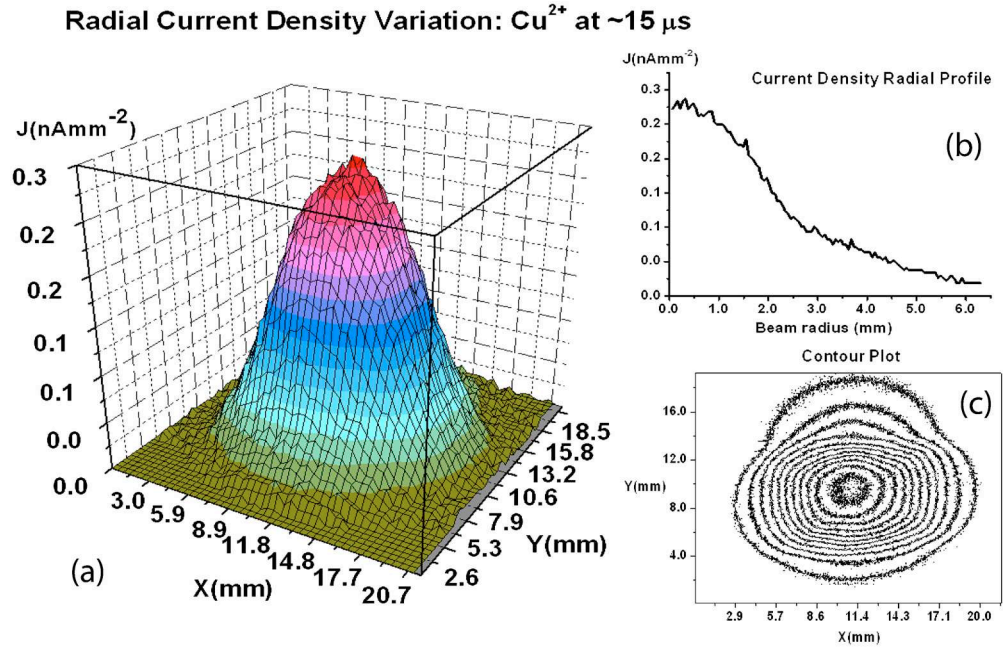

FIG. 9. (Color online) [(a)–(c)] Profile of the current density distribution over the Cu^{2+} ion bunch. The image is referenced to the current density peak in the TOF current recorded by the Faraday cup (Fig. 2). (b) Radial profile of the current density distribution. (c) Contour plot of the current density profile (a).

However, further increases in J with V_{ext} result in aberration of the plasma boundary, and in concert with the concomitant electric field distortion, overfocusing occurs so that ion bunches experience strong divergence upon injection into the drift tube. The resulting perveance mismatch manifests itself as a steep decrease in the perveance profile at high values of V_{ext}. The inset in Fig. 5 compares the perveance for $d=24$ mm (dc extraction 5–17 kV) and $d=12$ mm (pulsed extraction 17–40 kV). The smaller gap width in the case of pulsed extraction results from the requirement for a smaller value of d, if I_b is to continue to increase as V_{ext} increases (Child–Langmuir current density law). For pulsed extraction, beyond the turning point, the perveance displays a similar decay profile, however the rate of decay is less pronounced. Referring to Fig. 6, where the perveance for all charge states from Cu^+ to Cu^{5+} is plotted for values of $F=3.96$ kJ cm^{-2} and $V_{ext}=5-17$ kV dc, it can be readily observed that this behavior is replicated for all other extracted ion bunches.

Despite the fact that Eq. (9) predicts that the perveance P should increase as the square root of Z_i, the turning point in P actually decreases with increasing ion charge (cf., Fig. 6, inset). This can be explained in terms of distortion of the extraction field in the gap, resulting in perveance mismatch, and concomitant excessive lateral beam expansion, which

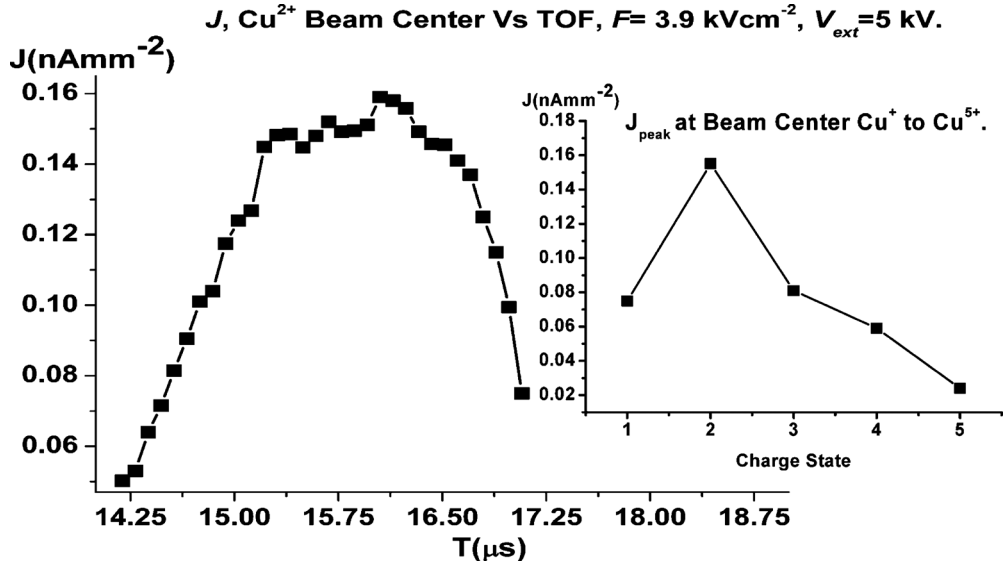

FIG. 10. Time resolved current density of the Cu^{2+} ion bunch, along the bunch centerline, i.e., along the axis of the drift tube. Inset: peak recorded current density, charge resolved for each ion bunch along the axis of the drift tube.

affects highly charged ions more than lowly charged ions. Hence the deleterious effects of perveance mismatch become apparent at lower values of extraction bias. This is a fundamental limitation in high pressure LIS designs and so it must be compensated for by employing extensive electrostatic optical systems for efficient beam transport. In a previous publication,[23] the peak collected current from the DCU-LIS increased by a factor of 8 after an Einzel lens array with appropriate bias values was employed.

V. EXTRACTED BEAM CURRENT DENSITY STRUCTURE

Figure 7 shows the time resolved current density recorded by a Faraday cup. The data were obtained at a dc extraction bias of 5 kV for a fluence of $F=3.96$ kJ cm^{-2}. The spatial distribution of the ions, within each charge resolved ion bunch, was also recorded with the aid of a gated intensified CCD camera (ICCD). The Faraday cup recorded the current (inset Fig. 7), which was subsequently converted to current density J using the outer diameter of each time resolved ion bunch image to estimate the appropriate area. The variation in areas along each bunch is displayed in Fig. 8 for Cu^+ to Cu^{5+}. The inset in Fig. 8 shows a time resolved mosaic of the ICCD images for the Cu^+ ion bunch with the upper quadrant removed to display the detected particle gradient. It is also clear from Fig. 8 that as the charge state increases, the temporal duration of the ion bunch decreases. It is clear that the outer diameter of each ion bunch also initially increases with degree of ionization, from Cu^+ to Cu^{3+} and then decreases from Cu^{3+} to Cu^{5+}.

To determine the actual spatial distribution of current density across a plane intersecting each ion bunch, a two dimensional intensity profile was recorded by the ICCD camera for the relevant time delay. The corresponding current density was obtained from the Faraday cup measurement. The current density scale for the 2D profile was adjusted so that the integrated current density corresponded to the Faraday cup measurement. Using this approach we determined the time-space resolved J distribution, see, e.g., Fig. 9, which shows the result of this procedure for Cu^{2+} at a time delay of 15.04 μs. The upper inset displays the radial profile of this 2D distribution and the lower inset a contour plot of the distribution. The procedure was repeated for all time delays covering the front to the tail of the bunch, i.e., ca. 14–18 μs (see Fig. 7, inset for the corresponding Cu^{2+} time trace).

The time resolved profile of the peak J at the beam center for the Cu^{2+} bunch is displayed in Fig. 10. It was noted that within the overall bunch duration of ~3 μs, a region 1.3 μs in duration exhibited a maximum/minimum variation of 10% on the peak recorded signal. Thus for approximately half of the Cu^{2+} beam duration, the current density at the beam center is nearly constant. If this procedure is repeated at the peaks of each charge resolved bunch (Fig. 2), then the charge dependent peak value of J at the beam center can be plotted. This result is shown in the inset of Fig. 10. As expected the peak J value at the center of each ion bunch displays approximately the same trend as the peak currents observed from the Faraday cup with the maximum beam-center current density recorded for the Cu^{2+} ion bunch.

From Fig. 9, approximately 75% of the beam current density resides within a radius of 4.2 mm of the beam center. Thus a cylinder, ~8.4 mm in diameter encloses an ion bunch of nearly constant charge density (<10% variation) along its major axis and varies by no more than 25% radially. To our knowledge this is the first report of the internal current density structure within an ion bunch for LIS systems.

The use of an aperture at the end of the system to block all but this section of the beam would allow packets of highly charged ions of almost uniform dose to be delivered to a target for implantation studies. Furthermore, energy compensating electrostatic elements (such as an ion energy analyzer with a wide aperture) could be used to minimize the kinetic energy dispersion within an ion bunch, thus shortening its temporal duration and increasing the peak current.

VI. CONCLUSION

The performance of the DCU-LIS, a compact, high-pressure laser ion source has been presented and discussed. The system perveance has also been measured and a pronounced turning point its profile, related to electric field distortion and strong lateral beam expansion, was observed. The peak current density at the beam center for all charge states from Cu^+ to Cu^{5+} has also been presented and ranged from 0.3 to 0.16 nA mm^{-2}. Finally the internal current density structure has been presented for Cu^{2+}.

ACKNOWLEDGMENTS

The authors wish to acknowledge Enterprise Ireland for financial support over the course of this project (Grant No. SC/2003/0180).

[1] N. J. Peacock and R. S. Pease, J. Phys. D **2**, 1705 (1969).
[2] B. Sharkov and R. Scrivens, IEEE Trans. Plasma Sci. **33**, 1778 (2005).
[3] M. Yoshida, J. Hasegawa, J. W. Kwan, Y. Oguri, M. Nakaima, K. Horioka, and M. Ogawa, Jpn. J. Appl. Phys., Part 1 **42**, 5367 (2003).
[4] J. Collier, G. Hall, H. Haseroth, H. Kugler, A. Kuttenberger, K. Langbein, R. Scrivens, T. R. Sherwood, J. Tambini, O. B. Shamaev, B. Yu. Sharkov, A. Shumshurov, S. M. Kozochkin, K. N. Makarov, and Yu. A. Satov, Rev. Sci. Instrum. **67**, 1337 (1996).
[5] D. Doria, A. Lorusso, F. Belloni, V. Nassisi, L. Torrisi, and S. Gammino, Laser Part. Beams **22**, 461 (2004).
[6] *Pulsed Laser Deposition of Thin Film*, edited by D. B. Chrisey and G. K. Hubler (Wiley, New York, 1994).
[7] S. Prawer, Diamond Relat. Mater. **4**, 862 (1995).
[8] H. T. Calligaro, J. Castaing, J.-C. Dram, B. Moignard, J. C. Pivin, G. V. R. Prasad, J. Salomon, and P. Walter, Nucl. Instrum. Methods Phys. Res. B **181**, 180 (2001).
[9] H. Homeyer, Nucl. Instrum. Methods Phys. Res. B **139**, 58 (1998).
[10] C. Davies, Rev. Sci. Instrum. **43**, 556 (1972).
[11] J. E. Osher and G. W. Hamilton, Symposium on Ion Sources and Formation of Ions Beams, Brookhaven National Laboratory, New York, October 1971, Paper No. BNL 50310.
[12] D. Aldcroft, J. Burcham, H. C. Cole, M. Cowlin, and J. Sheffield, Proceedings of the Fifth European Conference on Controlled Fusion and Plasma Physics, Euroatom CEA, Grenoble, France, 1972, Vol. 1, p. 106.
[13] T. H. Stix, Plasma Phys. **14**, 367 (1972).
[14] G. G. Kelley, O. B. Morgan, L. D. Stewart, W. L. Stirling, and H. K. Forsen, Nucl. Fusion **12**, 169 (1972).
[15] W. S. Cooper, K. H. Berkner, and R. V. Pyle, Nucl. Fusion **12**, 263 (1972).
[16] E. R. Harrison, J. Appl. Phys. **29**, 909 (1958).

[17]I. Langmuir and K. R. Blodgett, Phys. Rev. **24**, 49 (1924).
[18]E. Surrey and A. J. T. Holmes, Rev. Sci. Instrum. **61**, 2171 (1990).
[19]K. Y. Sung, W. Jeon, S. H. Chun, and E. H. Choi, 14th IEEE International Pulsed Power Conference 2003, 2003, Vol. 2, pp. 999–1002, Paper No. PPC-2003.
[20]T. G. Mihran, IEEE Trans. Electron Devices **14**, 201 (1967).
[21]M. Cavenago and G. Bisoffi, Rev. Sci. Instrum. **62**, 1970 (1991).
[22]P. Yeates, J. T. Costello, and E. T. Kennedy, Rev. Sci. Instrum. **81**, 043305 (2010).
[23]P. Yeates, J. T. Costello, and E. T. Kennedy, Plasma Sources Sci. Technol. **19**, 065007 (2010).
[24]V. Nassisi and A. Pedone, Rev. Sci. Instrum. **74**, 68 (2003).
[25]M. Trinczek, A. Werdich, V. Mironov, P. Guo, A. J. Gonzalez Martınez, J. Braun, J. R. Crespo Lopez-Urutia, and J. Ullrich, Nucl. Instrum. Methods Phys. Res. B **251**, 289 (2006).
[26]T. N. Hansen, J. Schou, and J. G. Lunney, Appl. Surf. Sci. **138–139**, 184 (1999).
[27]W. Lochte-Holtgreven, *Plasma Diagnostics* (AIP, New York, 1995).
[28]H. S. Uhm, E. H. Choi, and M. C. Choi, Phys. Plasmas **9**, 2850 (2002).
[29]R. K. Parker, R. E. Anderson, and C. V. Duncan, J. Appl. Phys. **45**, 2463 (1974).
[30]W. L. Howes, J. Appl. Phys. **37**, 438 (1966).
[31]R. C. Davidson, *Physics of Non-Neutral Plasmas* (Addison-Wesley, Redwood City, CA, 1990), Chaps. 8 and 9.
[32]J. W. Kwan, IEEE Trans. Plasma Sci. **33**, 1901 (2005).
[33]T. S. Green, Inst. Phys. Conf. Ser. **54**, 271 (1980).
[34]J. R. Coupland, T. S. Green, D. P. Hammond, and A. C. Riviere, Rev. Sci. Instrum. **44**, 1258 (1973).
[35]G. R. Brewer, *Focusing of Charged Particles II* (Academic, New York, 1967), pp. 23–122.
[36]M. Miller, D. Ing, and J. Britt, IRE **16**, 83 (1955) (translation).
[37]K. Ambrose, J. Electron. Control **13**, 545 (1962).
[38]M. Cavenago and G. Bisoffi, Rev. Sci. Instrum. **63**, 2857 (1992).
[39]A. Septier, *Focusing of Charged Particles I* (University of Michigan, Academic, New York, 1967).
[40]B. Piosczyk and G. Dammertz, Rev. Sci. Instrum. **55**, 1421 (1984).
[41]M. E. Abdel Aziz, F. W. Abdel Salam, M. H. Yalat, A. G. Helal, T. H. El-Khabeary, and N. T. El-Merai, Proceedings of the 13th National Radio Science Conference, NRSC'96, Cairo, Egypt, 19–21 March 1996, INSPEC Accession No. 5577047.
[42]K. Y. Sung, W. Jeon, S. H. Chun, and E. H. Choi, 14th IEEE International Conference, Pulsed Power Conference, 2003, Vol. 2, pp. 999–1002, Paper No. PPC-2003.
[43]C. Bastien, G. Faillon, M. Simon, Electron Devices Meeting, 1982 International, pgs. 190–194.
[44]R. Uhlemann and G. Wang, Rev. Sci. Instrum. **60**, 2879 (1989).
[45]M. Kisaki, K. Shinto, T. Kobuchi, A. Okamoto, S. Kitajima, M. Sasao, K. Tsumori, M. Nishiura, O. Kaneko, Y. Matsuda, M. Wada, H. Sakakita, S. Kiyama, and Y. Hirano, Rev. Sci. Instrum. **79**, 02C113 (2008).
[46]M. Yoshida, J. Hasegawa, S. Fukata, Y. Oguri, M. Ogawa, M. Nakajima, K. Horioka, S. Maebara, and M. Shiho, Nucl. Instrum. Methods Phys. Res. A **464**, 582 (2001).
[47]Y. Oguri, Phys. Rev. ST Accel. Beams **8**, 060401 (2005).